Evolution of stresses over conjugate faults in Hjalli-Ölfus, South Iceland

Revathy M. Parameswaran[1,2†*], Ingi Th. Bjarnason[1,3], and Bergthóra S. Thorbjarnardóttir[1]

[1]Institute of Earth Sciences, University of Iceland, Reykjavik, Iceland

[2†]Geophysical Institute, University of Alaska Fairbanks, Alaska, USA

[3]Nordvulc Volcanological Centre, Institute of Earth Sciences, University of Iceland, Reykjavik, Iceland

†Current affiliation

*Corresponding Author: Revathy M. Parameswaran (email: rmparameswaran@alaska.edu)

Supplementary Material

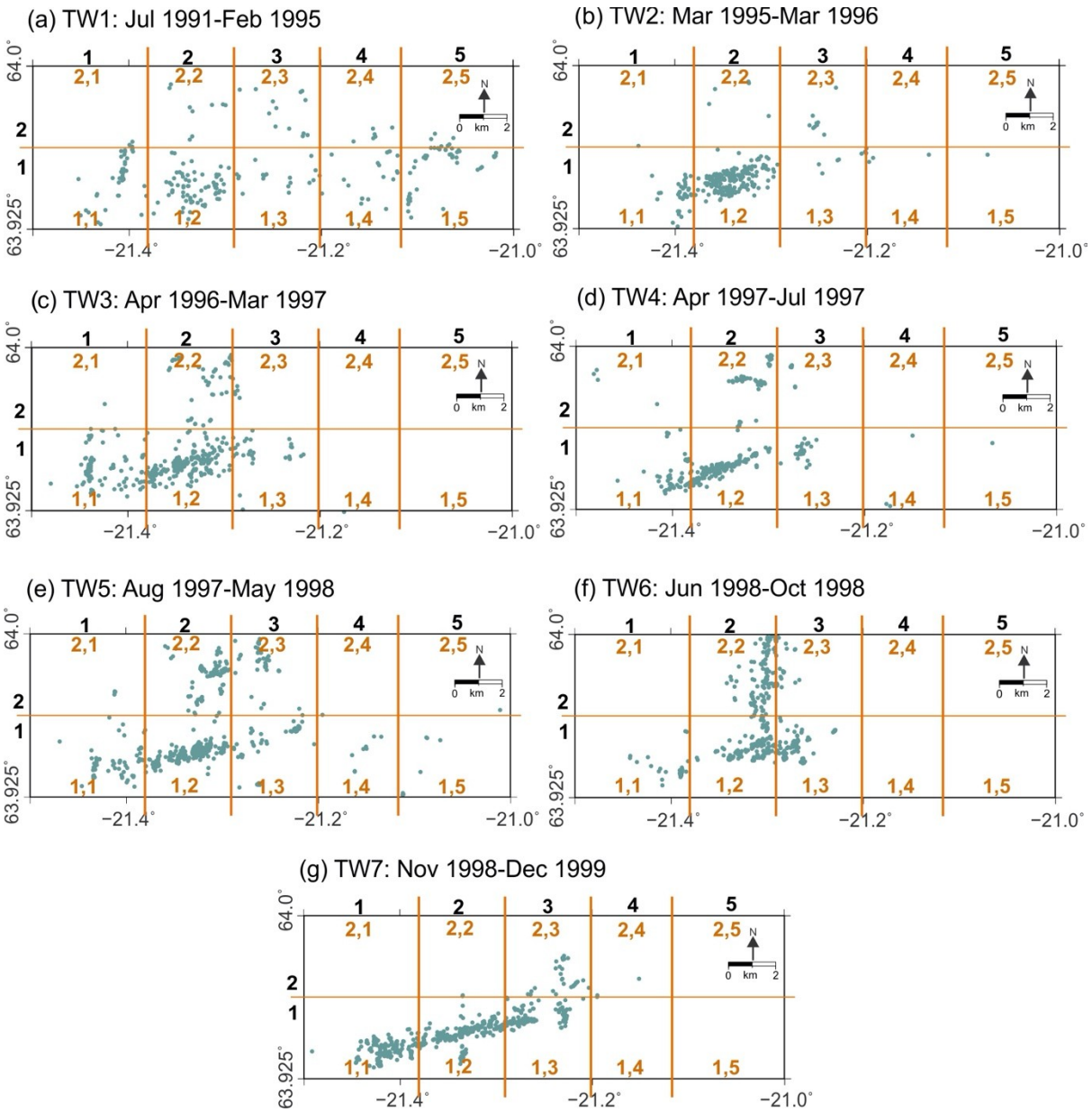

Supplementary Figure S1: *Grid-wise spatial distribution of selected events (polarities ≥ 4; amplitudes ≥ 12) from depths 0-10 km in (a) TW1, (b) TW2, (c) TW3, (d) TW4, (e) TW5, (f) TW6, and (g) TW7.*

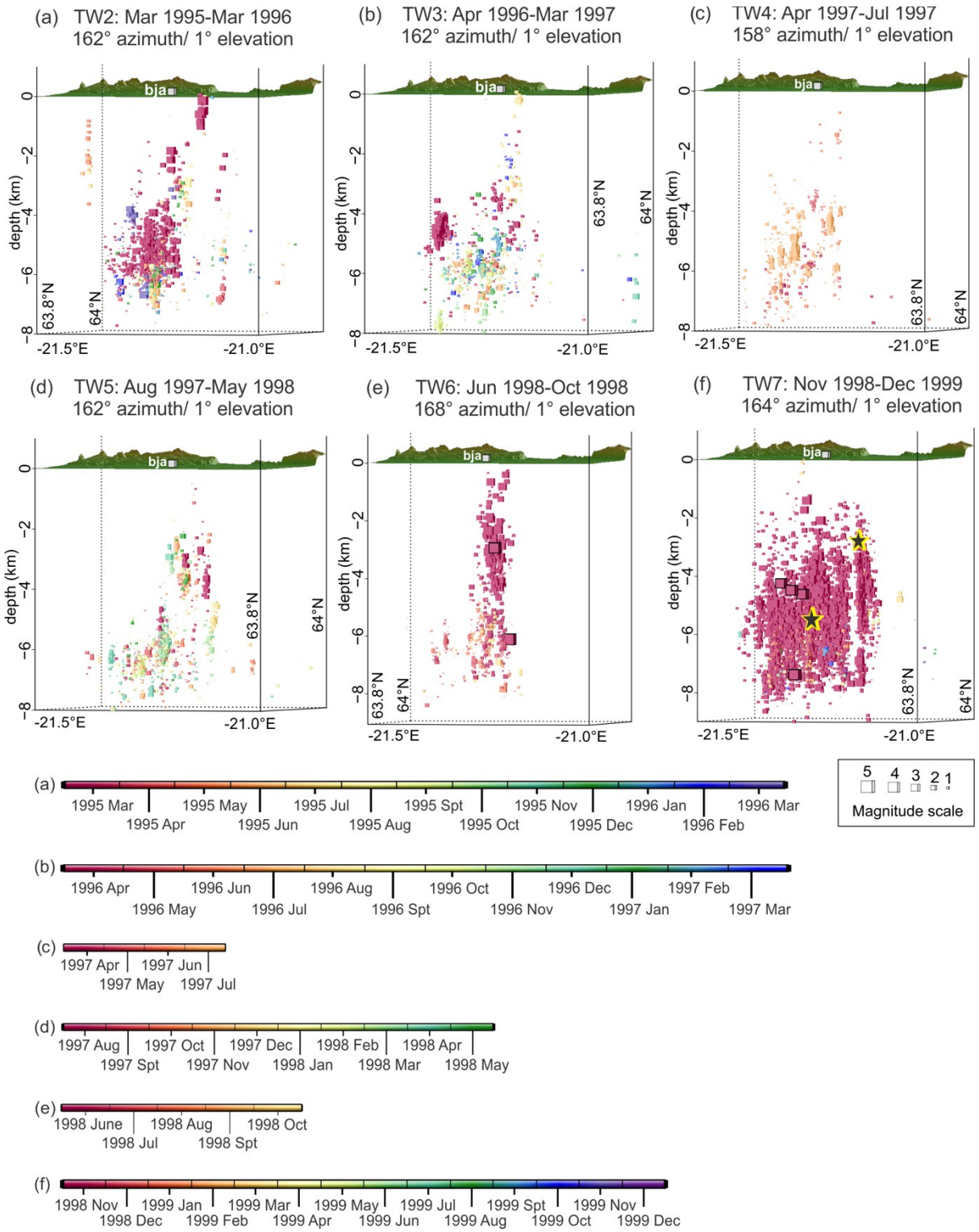

Supplementary Figure S2: *Depth distribution of all relocated events from TW2 to TW6 – (a) TW2, (b) TW3, (c) TW4, (d) TW5, (e) TW6, and (f) TW7 (after Parameswaran et al., 2020).*

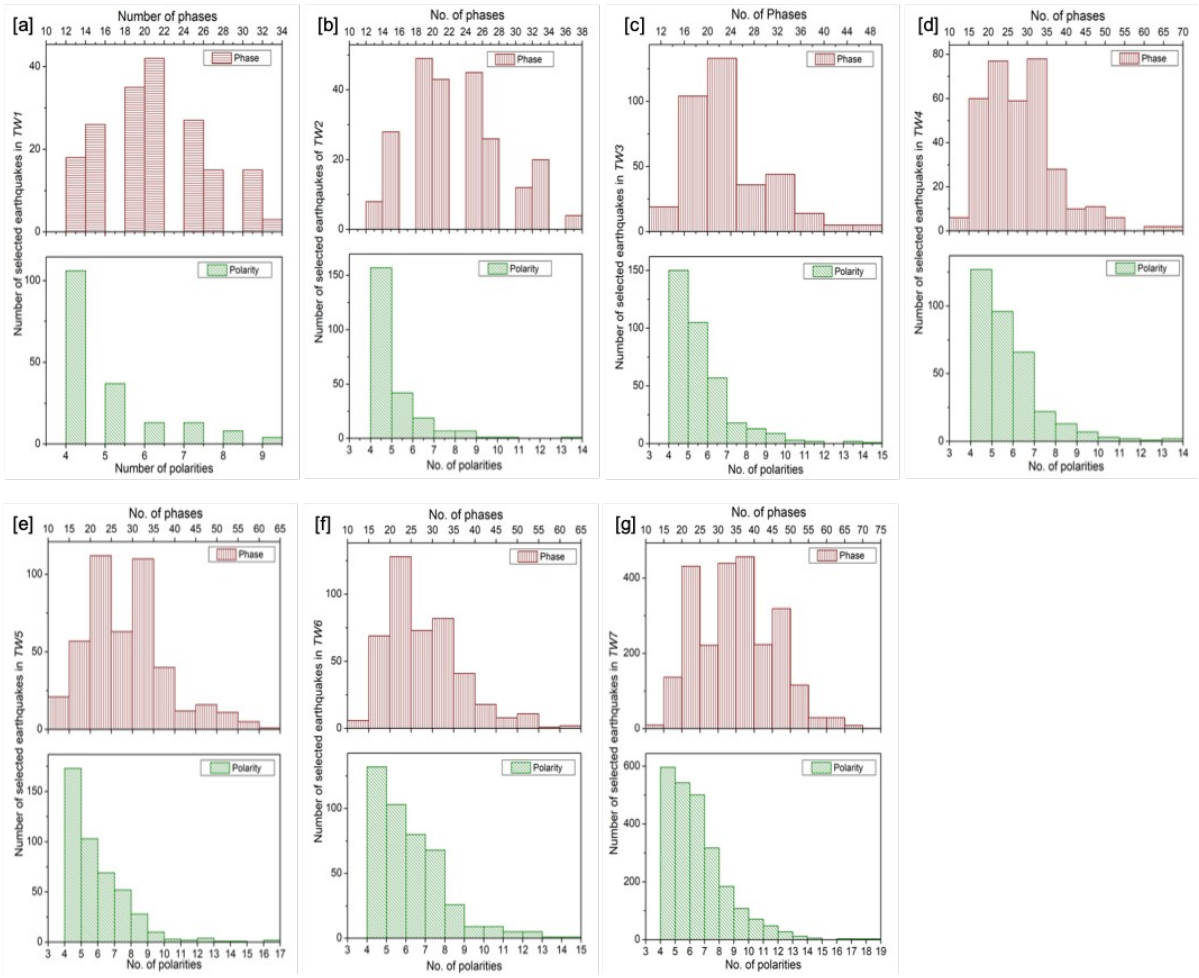

Supplementary Figure S3: ***Phase and Polarity histograms for:*** *(a) TW1, (b) TW2, (c) TW3, (d) TW4, (e) TW5, (f) TW6, and (g) TW7. In each subplot - Top: Histogram of phase amplitudes used to determine the fault plane solutions (FPSs) of 'selected events'; Bottom: Histogram of polarities used to determine the FPSs of 'selected events'.*

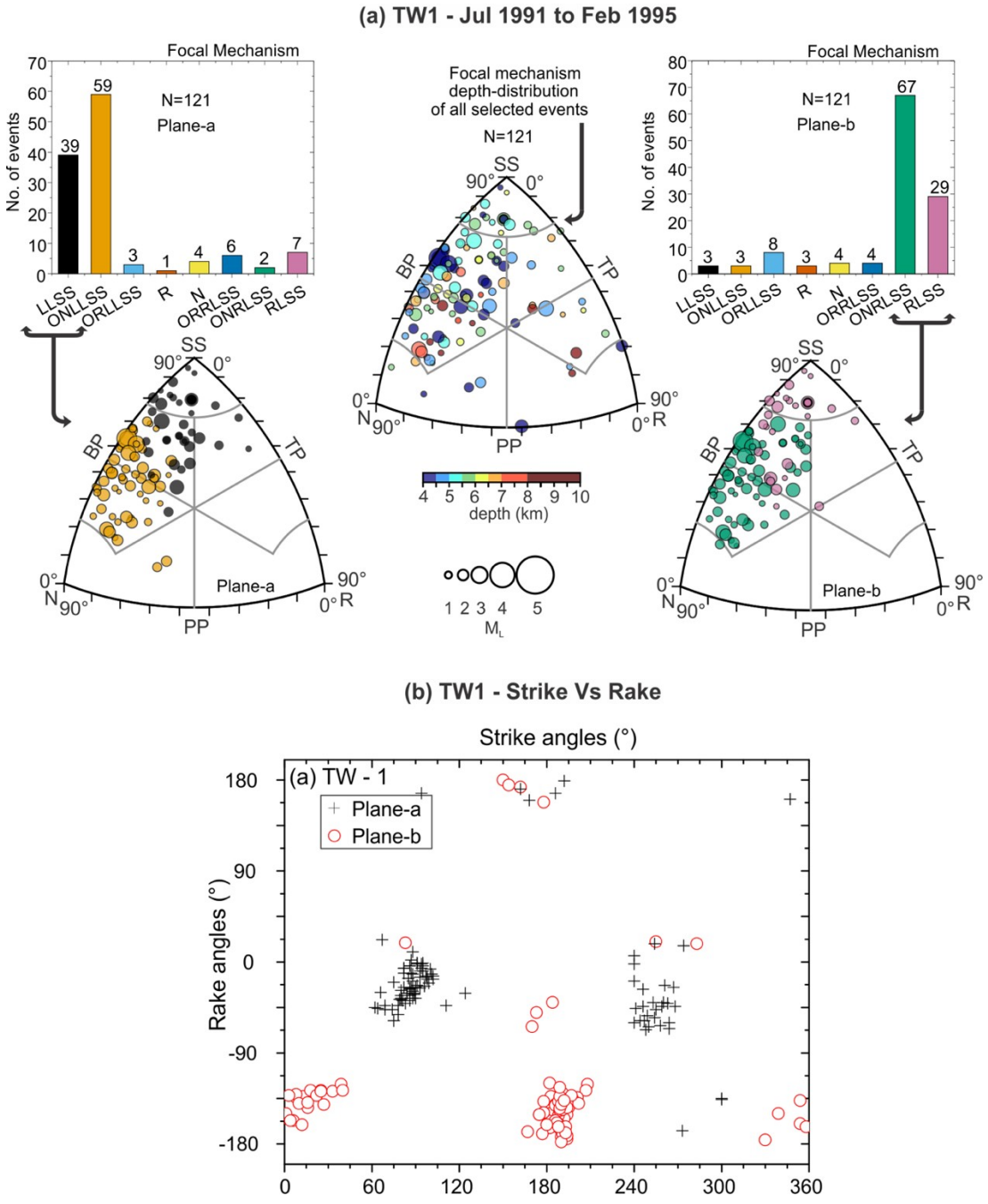

Supplementary Figure S4: *Analysis of selected focal plane solutions (FPSs) from TW1. (a) Rake analysis – bar diagrams show the abundance of different focal mechanisms present in the TW for both nodal planes (Plane-a and Plane-b). Ternary plots below the bar-diagrams illustrate the magnitudes of events in the two major types of faulting during TW1. The ternary plot at the center shows the magnitude- and depth- distributions of the selected events. (b) The scatter plot demonstrates the relation between the rake- and strike- angles of the selected events, for both nodal planes.*

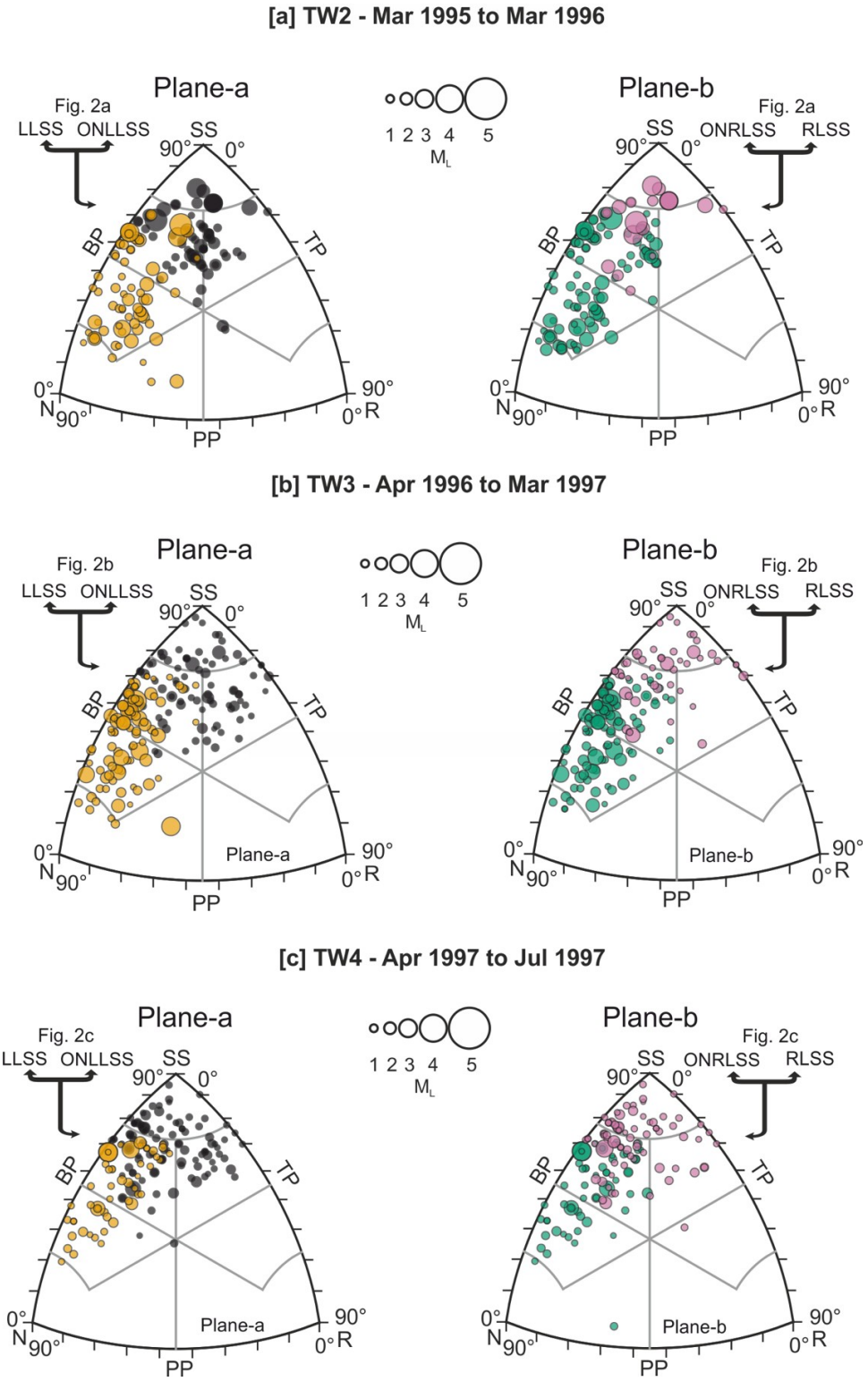

Supplementary Figure S5: *Left and Right ternary plots show focal mechanism and magnitude distribution of dominant faulting styles in (a) TW2, (b) TW3, and (c) TW4, following the bar diagrams in Figure 2 of the manuscript. BP, TP, and PP stand for B-, T-, and P-axes plunges. R: Reverse, N: Normal, SS: Strike-slip.*

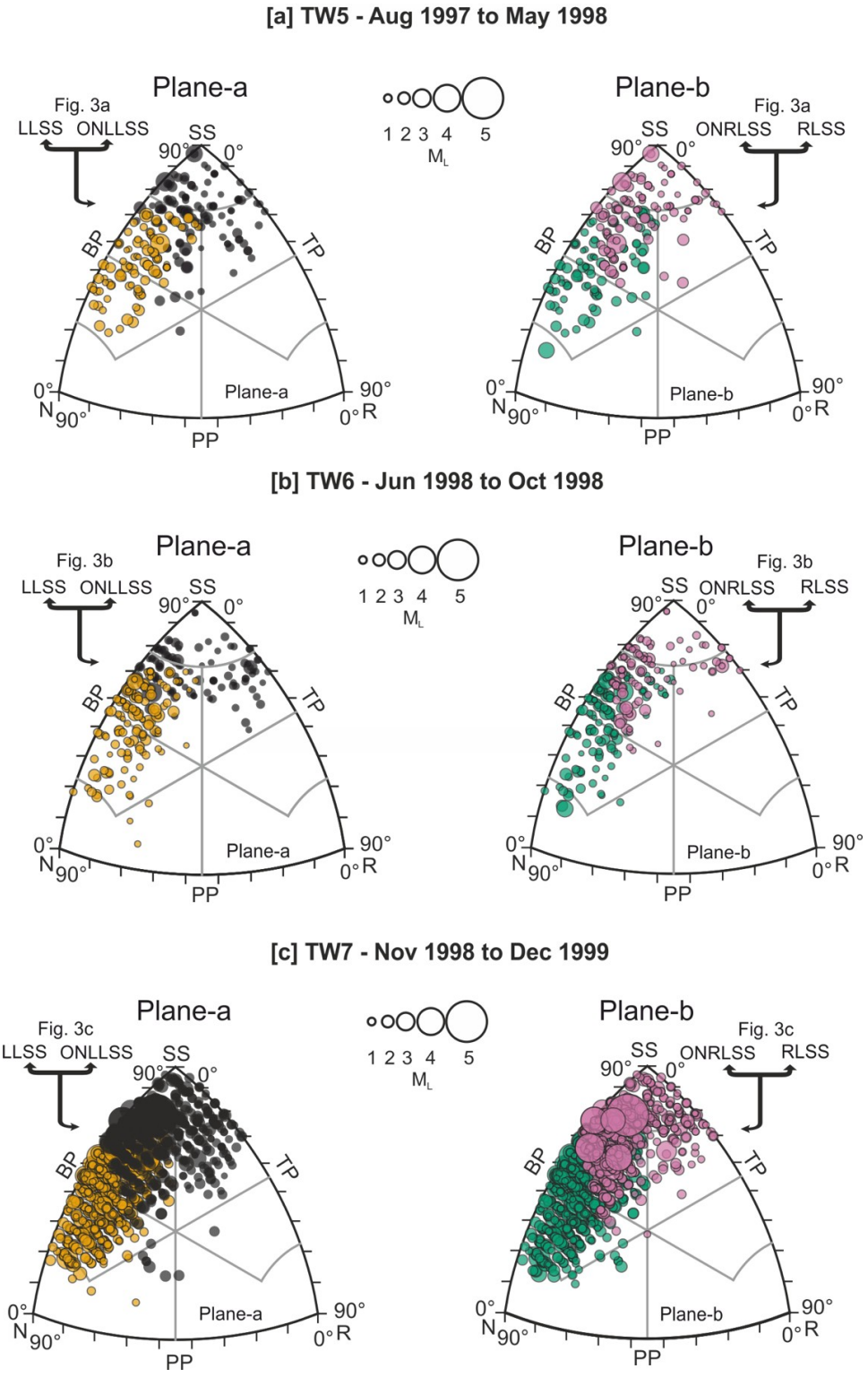

Supplementary Figure S6: *Left and Right ternary plots show focal mechanism and magnitude distribution of dominant faulting styles in (a) TW5, (b) TW6, and (c) TW7, following the bar diagrams in Figure 3 of the manuscript. BP, TP, and PP stand for B-, T-, and P-axes plunges. R: Reverse, N: Normal, SS: Strike-slip.*

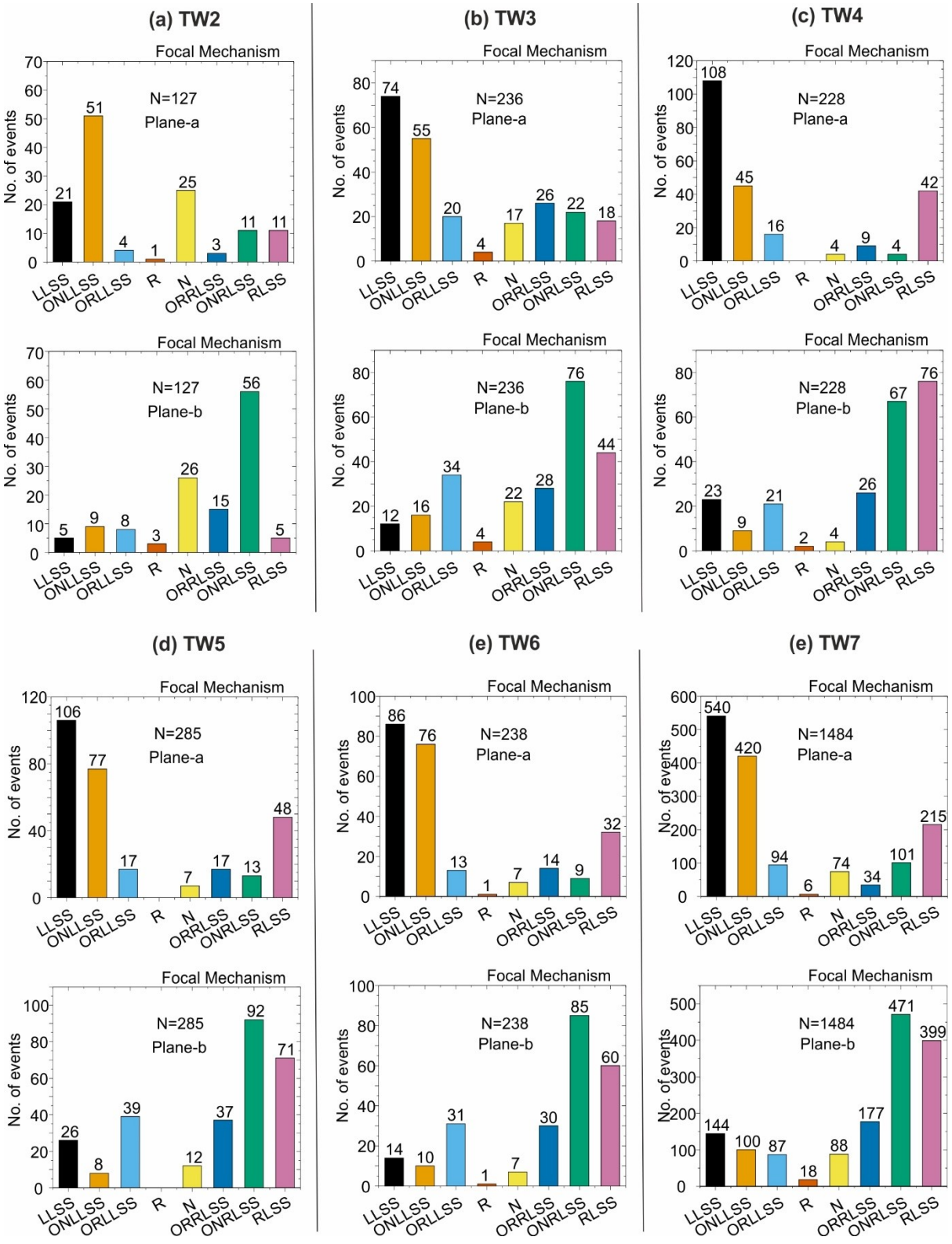

Supplementary Figure S7: *Rake analysis using bar-diagrams for both nodal planes of events with FPSs that don't align with prominent seismic trends (Figure 1f) for (a) TW2, (b) TW3, (c) TW4, (d) TW5, (e) TW6, and (f) TW7.*

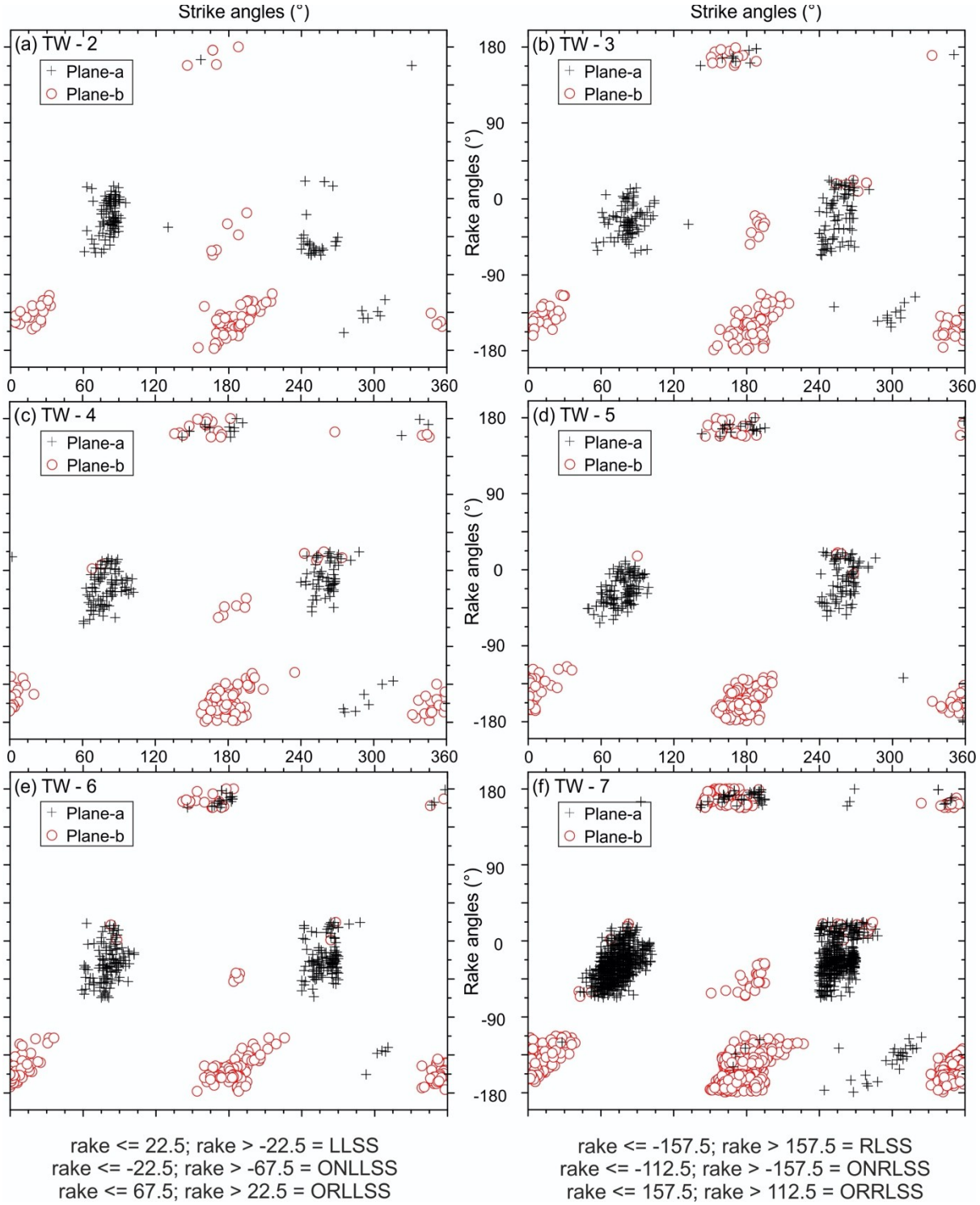

Supplementary Figure S8: *Scatter plots comparing the strike- and rake-distributions of Planes-a and -b of selected events in (a) TW2, (b) TW3, (c) TW4, (d) TW5, (e) TW6, (f) TW7. This analysis shows that majority of ~N-S striking nodal planes have right-lateral sense of motion, while majority of ~ENE-WSW planes have left-lateral sense of motion.*

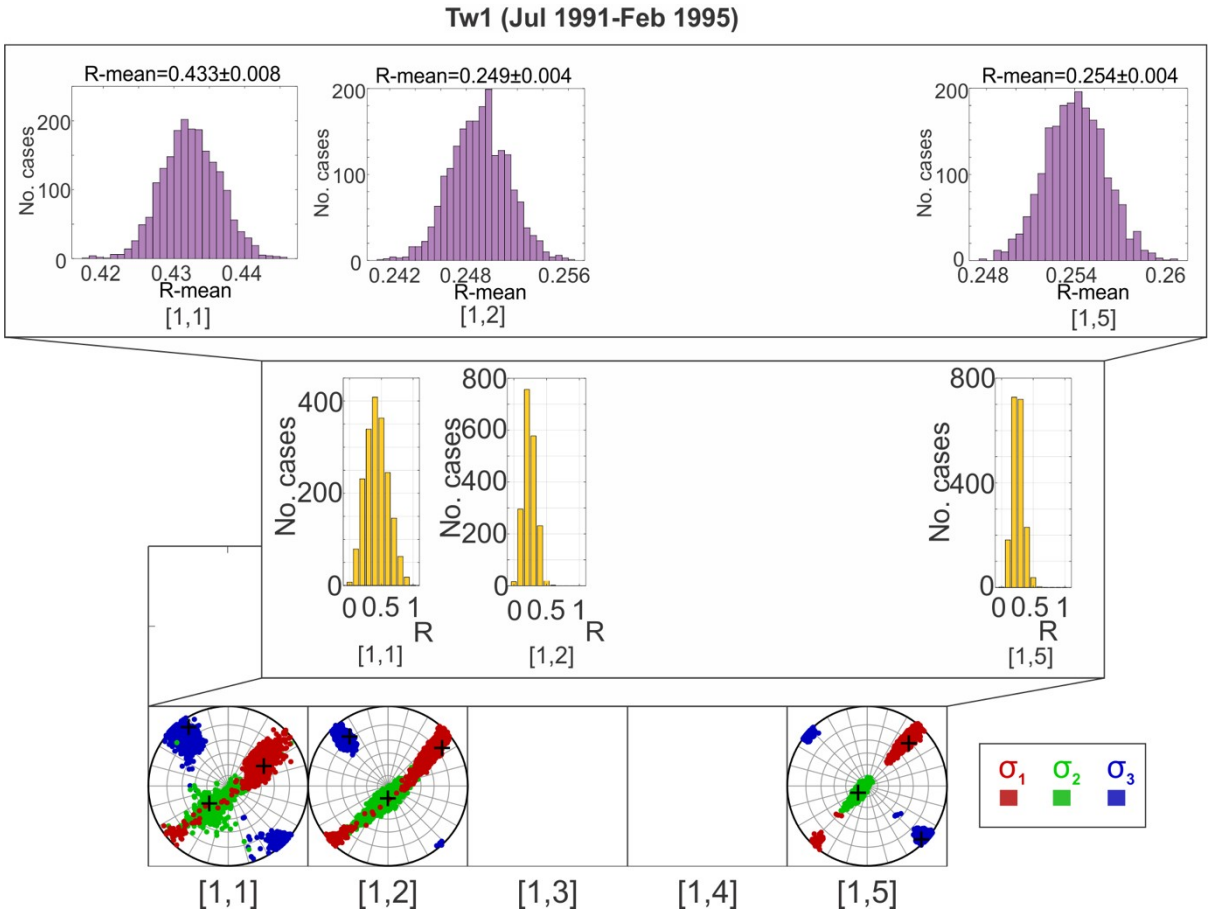

Supplementary Figure S9: *Stress inversion for selected events in TW1 showing distributions of principal stress axes in different grids. Yellow bar diagrams show the bootstrapped R-value distribution. Lavender bar diagrams illustrate bootstrapped R-mean of the computed R-values. '+' sign in each uncertainty lobe stands for the corresponding best-fit principal stress axes.*

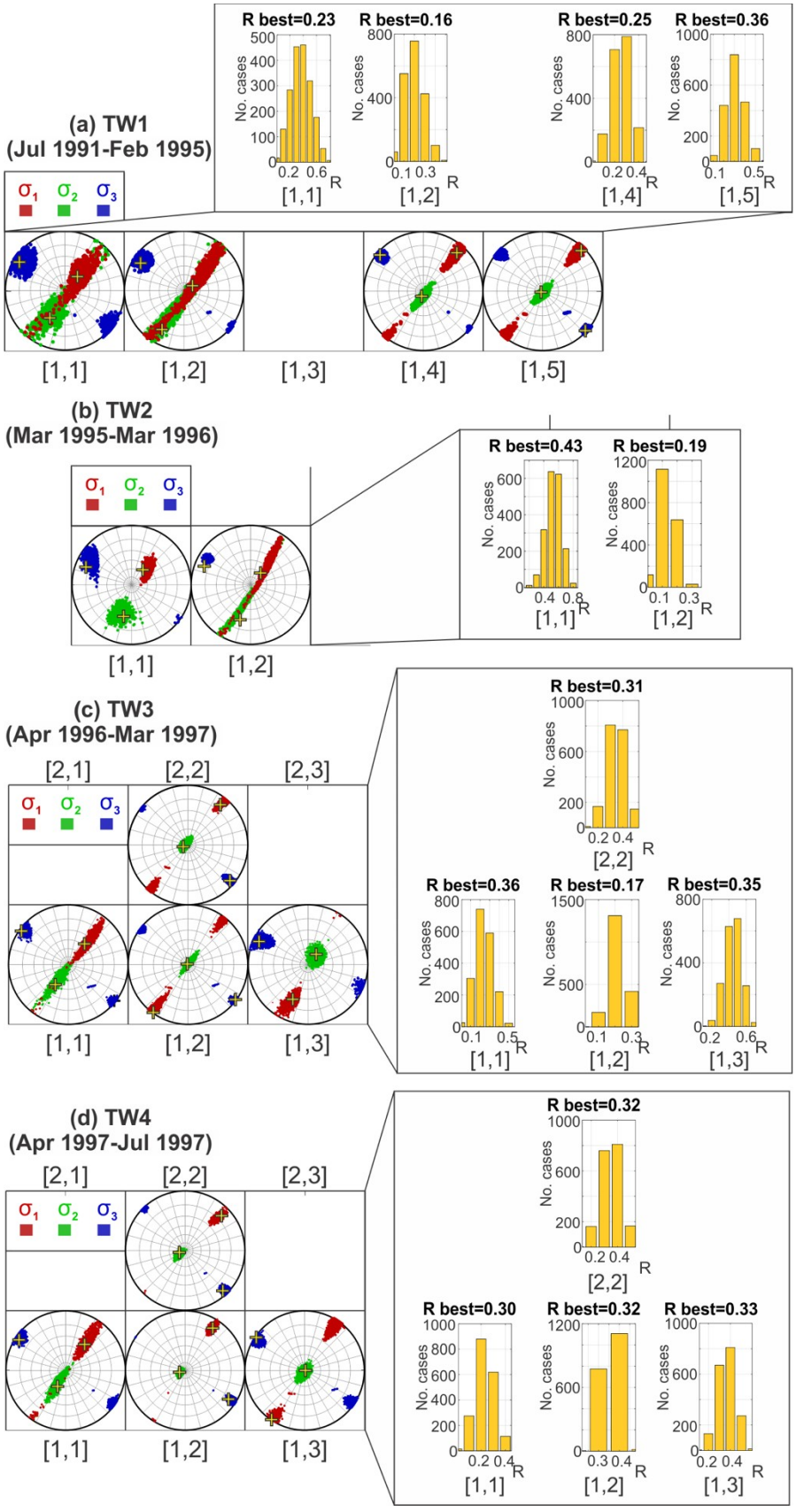

Supplementary Figure S10: *Stress inversion for all relocated events in (a) TW1, (b) TW2, (c) TW3, and (d) TW4. Yellow bar diagrams and '+' sign are as described previously.*

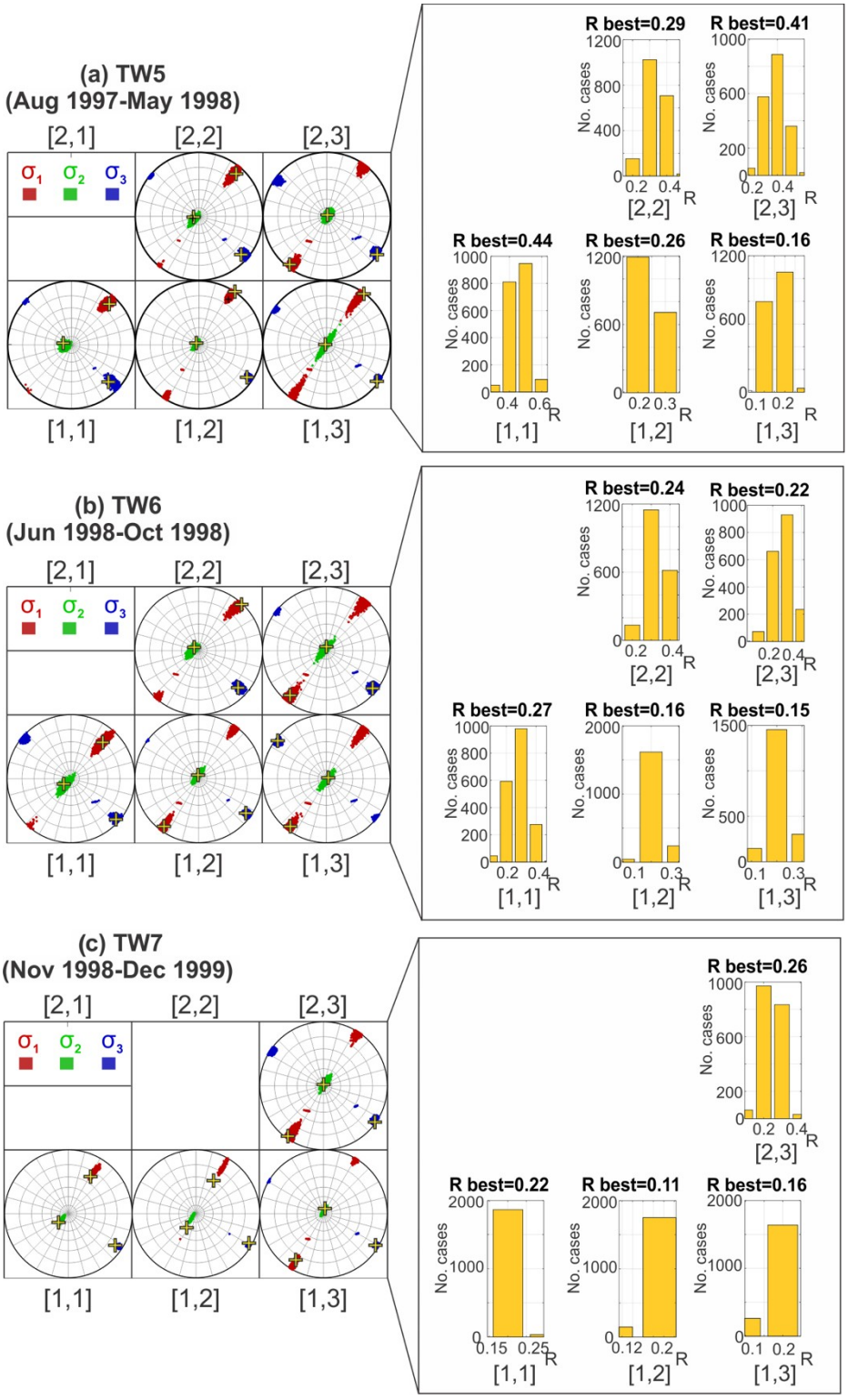

Supplementary Figure S11: *Stress inversion for all relocated events in (a) TW5, (b) TW6, and (c) TW7. Yellow and Lavender bar diagrams, and '+' sign – as described previously.*

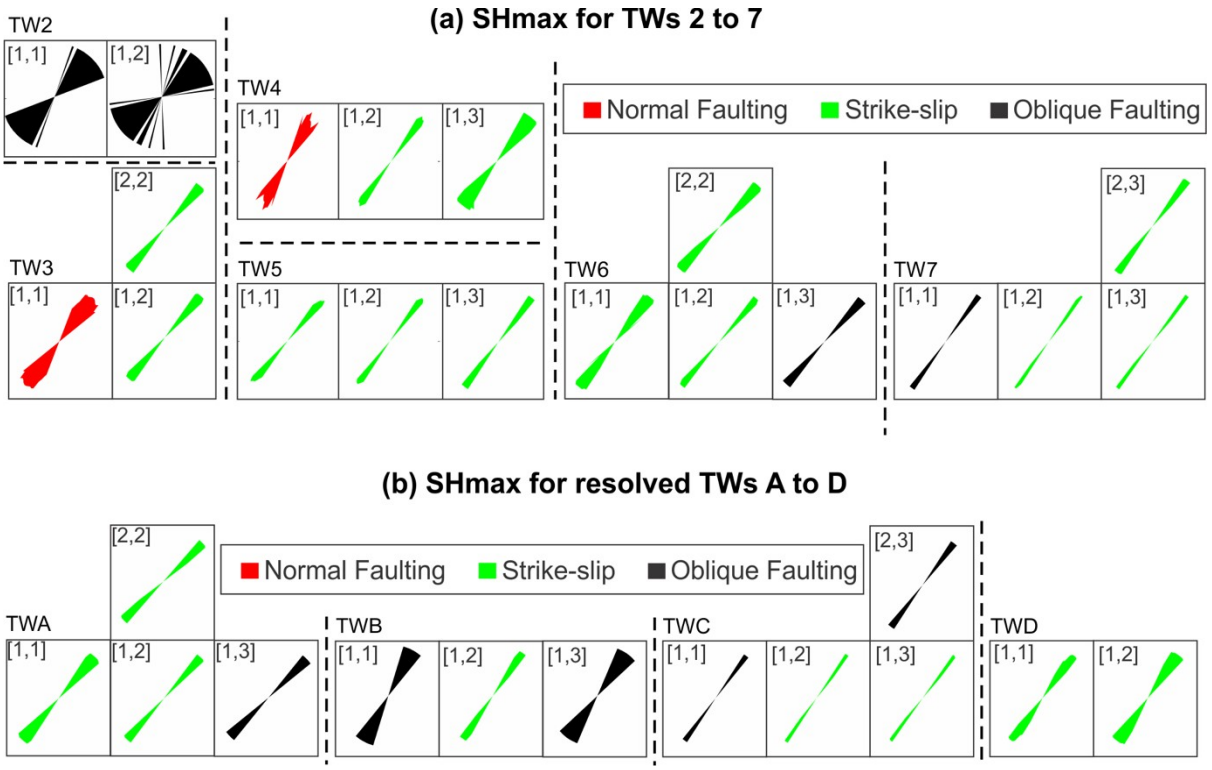

Supplementary Figure S12: SHmax orientations for TWs 2-7 and resolved TWs A-D: *(a) SHmax orientation distributions for all active grids in TWs 2-7. (b) SHmax orientation distributions for all active grids in resolved TWs A-D. The best-fit SHmax orientations and their confidence limits are listed in Supplementary Table S4.*

Supplementary Tables

S. No.	Significant south Iceland earthquakes	Catalogue
1	2013 Mw 5.2	GCMT
2	2000 mB 5	BJI
3	2003 Mw 5.3	HRVD
4	1998 Mw 5.1	HRVD
5	1998 Mw 5.4	HRVD, SIL
6	1997 mB 5	BJI
7	2008 Mw 6.3	GCMT
8	2000 Mw 6.4	SIL
9	2000 Mw 6.5	SIL

Supplementary Table S1: *List of numbered earthquakes marked indicated by white numbers (red stars) in Figure 1b.*

Rake angle	Type of faulting	Acronym
22.5° ≥ rake > − 22.5°	Left-lateral strike-slip	LLSS
−22.5° ≥ rake> −67.5°	Oblique–normal left–lateral strike-slip	ONLLSS
− 67.5° ≥ rake > − 112.5°	Normal	N
− 112.5° ≥ rake > − 157.5°	Oblique–normal right–lateral strike-slip	ONRLSS
− 157.5° ≥ rake > 157.5°	Right-lateral strike-slip	RLSS
157.5° ≥ rake > 112.5°	Oblique–reverse right–lateral strike-slip	ORRLSS
112.5° ≥ rake > 67.5°	Reverse	R
67.5° ≥ rake > 22.5°	Oblique–reverse left–lateral strike-slip	ORLLSS

Supplementary Table S2: *Criteria for rake-based classification of selected events into faulting-types (based on Rickard, 1972; Aki and Richards, 1980; e.g., White et al., 2009).*

TWs as in Figure 6 and Sup. Figure S12b	Active Grids	R-mean with 95% confidence level		
		1	2	3
A	2	-	0.360 ± 0.003	-
	1	0.258 ± 0.004	0.258 ± 0.002	0.189 ± 0.002
B	2	-	-	-
	1	0.207 ± 0.004	0.144 ± 0.002	0.185 ± 0.003
C	2	-	-	0.157 ± 0.002
	1	0.175 ± 0.001	0.156 ± 0.0008	0.165 ± 0.001
D	2	-	-	-
	1	0.195 ± 0.003	0.211 ± 0.003	-

Supplementary Table S3: *Grid-wise R-mean values for resolved TWs A-D shown in Figure 6 and Supplementary Figure S12b.*

TWs as in Figures 4 and 5	Active Grids	Best-fit SHmax and σ_3 orientations (in °)					
		1		2		3	
		SHmax	σ_3	SHmax	σ_3	SHmax	σ_3
2 (Mar 1995-Mar 1996)	2	-	-	-	-	-	-
	1	**[52.88]** *Min= 18.7 Max= 68.6*	*[-46.28] [(133.72)] Min = -62.5 Max = -33.1*	**36.27** *Min= -2.2 Max= 82.3*	*-54.43 (125.57) Min = -54.8 Max = -41*	-	-
3 (Apr 1996-Mar 1997)	2	-	-	**42.78** *Min= 35.4 Max= 47.2*	*132.40 Min = 125.2 Max = 133.7*	-	-
	1	**37.35** *Min= 21.3 Max= 51.4*	*127.59 Min = 120.3 Max = 135.4*	**42.75** *Min= 35.6 Max= 48.0*	*132.82 Min = 124.6 Max = 134.3*	-	-
4 (Apr 1997-Jul 1997)	2	-	-	-	-	-	-
	1	**32.27** *Min= 19.3 Max= 40.9*	*123.09 Min = 109.5 Max = 129.5*	**40.14** *Min= 31 Max= 48.0*	*130.07 Min = 120.7 Max = 131.0*	**41.94** *Min= 28.9 Max= 48.2*	*131.57 Min = 116.6 Max = 135.1*
5 (Aug 1997-May 1998)	2	-	-	-	-	-	-
	1	**46.27** *Min= 34.8 Max= 46.3*	*137.27 Min = 125.2 Max = 137.27*	**41.2** *Min= 32.6 Max= 41.2*	*131.76 Min = 122.8 Max = 131.76*	**39.00** *Min= 33.1 Max= 41.3*	*128.83 Min = 123.5 Max = 132.0*
6 (Jun 1998-Oct 1998)	2	-	-	**47.52** *Min= 36.9 Max= 49.8*	*136.77 Min = 126.4 Max = 136.77*	-	-
	1	**39.15** *Min= 30.2 Max= 50.6*	*129.67 Min = 121.4 Max = 132.7*	**40.4** *Min= 36.9 Max= 45.4*	*130.58 Min = 125.2 Max = 132.4*	**42.55** *Min= 36.9 Max= 46.9*	*132.77 Min = 126.5 Max = 135.0*
7 (Nov 1998-Dec 1999)	2	-	-	-	-	**38.64** *Min= 32.1 Max= 43.0*	*128.03 Min = 124.7 Max = 130.2*
	1	**37.58** *Min= 33.2 Max= 39.1*	*127.68 Min = 124.3 Max = 130.5*	**33.99** *Min= 33.2 Max= 38*	*124.43 Min = 123.7 Max = 127.6*	**38.04** *Min= 34.5 Max= 40.4*	*128.19 Min = 124.7 Max = 129.5*
TWs as in Figure 6	**Active Grids**	1		2		3	
		SHmax	σ_3	SHmax	σ_3	SHmax	σ_3
A (4 Jun 1998- 13 Aug 1998)	2	-	-	**49.89** *Min= 40.5 Max= 51.9*	*139.76 Min = 130.2 Max = 141.1*	-	-
	1	**42.93** *Min= 33.2 Max= 49.3*	*132.62 Min = 123.8 Max = 137.7*	**44.74** *Min= 37.1 Max= 47.4*	*135.07 Min = 127.9 Max = 136.5*	**47.17** *Min= 39.2 Max= 51.3*	*-42.63 (137.4) Min = -51.2 Max = -40.1*

Supplementary Table S4: *Grid-wise best-fit SHmax and σ_3 orientations for TWs 2-7 and resolved TWs A-D, based on stress inversions shown in Figures 4,5 and Supplementary Figure S12. Strikes are measured clockwise from the north. Equivalent angles are listed in ( ) brackets. Numbers in* **[]** *are not used in calculations for average trends. Values in red indicate the best-fit values. 'Min' and 'Max' stand for the minimum and maximum values for SHmax and σ_3 orientations in each grid.*